Bioinspired Reversible Interlocker Using Regularly Arrayed High Aspect-Ratio Polymer Fibers

*Changhyun Pang, Tae-il Kim, Won Gyu Bae, Daeshik Kang, Sang Moon Kim, and Kahp-Yang Suh**

The efforts to learn and take inspiration from nature have impacted virtually on every scientific area, leading to epidermal electronics,[1] biomimetic attachments,[2–5] optical systems,[6,7] and materials.[8,9] In addition, reversible binding or interlocking is an attractive feature that nature can provide and is enabled by a number of different intermolecular, capillary, electric, and mechanical forces. Examples are found in many biological systems, including parasites, insects, plant spreading, and bird feathers.[10]

In addition, nature has created unique structural devices with specially designed physical structures such as interlocking between "hooks" and "loops" in burdock's seeds (now commonly used in the fabric Velcro)[11] and the wing-to-body locking device in beetles.[12] Although the binding mechanism is relatively simple, miniaturization of the hook-and-loop type mechanical interlocking in Velcro tape is not straightforward since the fabrication of such structures on a small scale is challenging, even with the current fabrication techniques. The wing-locking device in beetles is operated by bringing densely populated microhairs (termed microtrichia) on the cuticular surface in contact. This interlocking is adapted to fix the wing of insects by maximizing lateral shear friction while minimizing vertical lift-off during numerous cycles of folding and unfolding states. Despite some earlier observations on the existence of wing locking devices in beetles,[12] several issues have not been explored concerning the underlying mechanism of reversible binding and its potential applications to flexible and reversible interlockers.

Recently, core/shell type nanowires and carbon nanotube (CNT) based carbon forests have been introduced as a permanent or reversible adhesive between two surfaces.[13,14] We report here that regularly ordered high aspect-ratio (AR) polymer fibers can also be used as a reversible interlocker because of the amplification of van der Waals forces. Unlike inorganic nanowires and CNTs, the geometry (e.g., length and width), layout density, and material properties of polymer hairs can be tuned precisely so as to tailor athe dhesion force of mechanical interlocking. In addition, a layered interlocking device could provide optimal operating conditions for shear adhesion since the contact is made via numerous tiny hairs present on two flexible surfaces and the lift-off is extremely simple and effortless by peeling off one of the layers in contact.

To investigate multiscale interlocking behaviors of high-AR hairs (or pillars) we used three polyurethane (PU)-based materials of different rigidity (elastic modulus: ≈3 MPa to 10 GPa). Using these materials, various pillar arrays were fabricated with three different radii (50 nm, 1.5 μm, and 15 μm) and aspect ratios (3, 6, and 10), for a total of 27 experimental sets. We found that the interlocking is mediated by attractive van der Waals forces, which can be significantly amplified by the presence of high-density micro- or nanohairs. Especially, the maximum shear locking force of ≈40 N cm^{-2} was observed for the nanopillar arrays of 50 nm radius and 1 μm height (AR = 10), which appears to show the highest adhesion strength among the polymer adhesives reported to date.

Figure 1a–c shows photographs of the beetle (Promethis valgipes) and its anterior field of thorax, which contains dense, hexagonal microhair arrays of approximately 0.9 μm radius and 18 μm height with the spacing ratio, i.e., the distance between hairs divided by width, of ≈3. When these hairs are interconnected, a high shear locking force is expected to occur, as shown schematically in the left bottom panel of Figure 1d, while a normal lift-off would be simple and effortless. This wing-locking device is highly reversible and does not require additional physical load or surface modification. A close examination in Figure 1c reveals that the microhairs are slightly bent in one direction, allowing for pointed directionality along a particular spatial axis. The primary function of these microhairs is to reversibly lock the wing of beetles, whose contact is continuously monitored by conjunctive sensory organs (see Supporting Information for details). In addition, this wing-locking device is known to protect delicate flight wings by dehydration of nanopore channels from air drying.[12] The microhairs are made of β-keratin, whose elastic modulus and Hamaker constant were reported to be ≈2 GPa and ≈10×10^{-20} J, respectively.[15]

To demonstrate multiscale interlocking behaviors by van der Waals interactions, we tested a variety of hairy structures with different structural dimensions and material properties. After preparing silicon masters with suitable geometry, the polymer hairs were fabricated by replica molding technique (see Experimental Section). Here, three polymer materials of different rigidity were used: PU (polyurethane elastomer, elastic modulus: 3 MPa), s-PUA (soft polyurethane acrylate, MINS 301 RM, elastic modulus: 19.8 MPa), and h-PUA (hard polyurethane

C. Pang, Dr. T.-i. Kim, D. Kang, S. M. Kim, Prof. K.-Y. Suh
Division of WCU Multiscale Mechanical Design
School of Mechanical and Aerospace Engineering
Seoul National University
Seoul 151-742, Korea
E-mail: sky4u@snu.ac.kr
W. G. Bae
Interdisciplinary program of Bioengineering
Seoul National University
Seoul 151-742, Korea

DOI: 10.1002/adma.201103022

ADVANCED MATERIALS
www.advmat.de

www.MaterialsViews.com

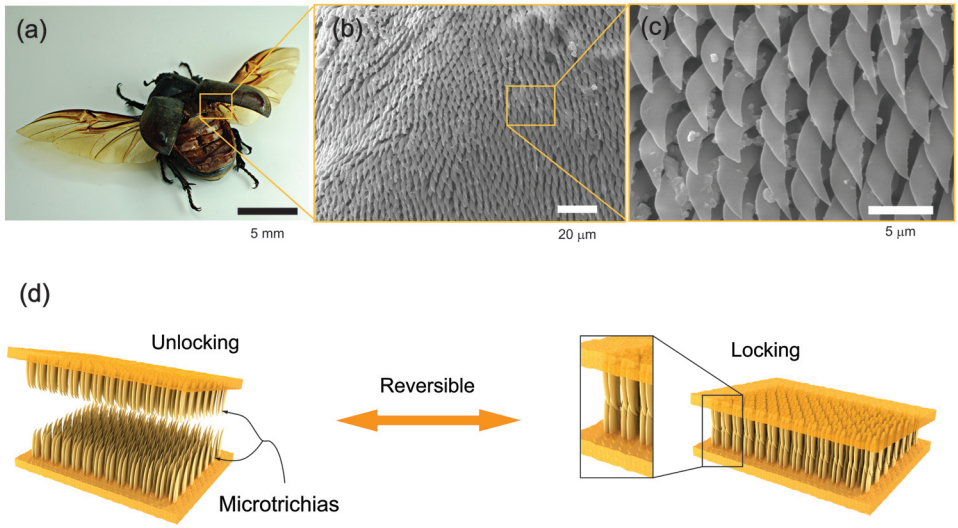

Figure 1. a) Photographs of the wing-locking device of the beetle (*Promethis valgipes*). b,c) SEM images of microtrichia on the cuticular surface with two different magnifications. d) Schematic of folding and unfolding states of wing-locking device.

acrylate, MINS RM 311, elastic modulus: ≈350 MPa to 10 GPa) (see **Table 1**).[16] Therefore, the modulus spans three orders of magnitude. Using these materials, various pillar arrays were prepared with the radius ranging from 50 nm to 15 μm (three orders of magnitude difference). For each pillar array, three different ARs (AR = height/diameter = 3, 6, and 10) were used, thus giving the total of 27 experimental sets. The tilted scanning electron microscopy (SEM) images of replicated polymer structures are shown in **Figure 2**a, demonstrating that the structures have high structural fidelity and integrity. Here, each group (column) was classified depending on the radius of hairs, which was 50 nm, 1.5 μm, or 15 μm. For consistency, all hairy structures had the same spacing ratio of three with the hexagonal packing geometry. The interlocking layers could be formed over a large area (9 × 13 cm^2) in a single replication step (see Supporting Information Figure S1).

The maximum shear locking forces were measured using custom-built equipment with a preload of 10 N cm^{-2} at the relative humidity 50% until a failure occurred (Figure 2b). Several notable findings are derived from the experiment. First, a smaller radius yielded a higher shear force, which was valid for all ARs and mechanical moduli shown in Figure 2b. Since a small radius is equivalent to a higher hair density and thus a higher number of hair-to-hair interlocking contacts per unit sample area, it is directly related to a higher adhesion force. Second, the shear strength increased with the decrease of elastic modulus and the increase in AR for all hairy structures tested. In particular, the nanohairs of 50 nm radius and 1 μm height showed the best shear locking force of ≈40 N cm^{-2} for intermediate modulus (19.8 MPa), which is presumably the highest shear strength among the polymer-based dry adhesives reported to date (see Supporting Information Figure S2).[17] For comparison, the maximal adhesion forces of typical Velcro and gecko-like polymer-based dry adhesives were reported to be ≈15 N cm^{-2} [18] and ≈26 N cm^{-2},[17] respectively. In contrast, the microhairs of 1.5 μm radius and 18 μm height, the scale of which is often found in many insects,[12] showed the maximum adhesion of ≈17 N cm^{-2} for low modulus (3 MPa), suggesting that softer hairs lead to a higher shear adhesion force for a given geometry. Third, the maximum shear adhesion was limited by replication capability of hairy structures. Namely, there was a certain limit in replicating high-AR structures due to collapse or mating between neighboring hairs.[20] This explains why some shear adhesion data (nanohairs of radius 50 nm and microhairs of radius 1.5 μm) are missing, and nanohairs of the intermediate modulus provided the maximum shear force instead of the PU elastomer in Figure 2b. The inset SEM images in Figure 2b provide an insight into how the interlocking contact is mediated by multiscale hairy structures. Here, the red arrows indicate the locations where complete interconnections had been made with overlapped hairs. The ratio of the overlapping was estimated to be ≈65 to 75%, regardless of the rigidity of the hairs, with some broken and misaligned hairs.

To investigate the durability of the interlocker presented here, the interlocking shear adhesion force was measured by using the nanohairs of 50 nm radius and 1 μm height over multiple cycles of reversible attachment and detachment with or without a thin coating of Pt (Supporting Information Figure S3).[20] Here, two coating thicknesses were used (5 and 10 nm) in order to evaluate the effect of elevated Young's modulus. It was found that these interlocking layers, when mechanically reinforced with a thin Pt coating, allow for noiseless and repeatable

Table 1. Summary of material properties used in the experiment: elastic modulus (E), Hamaker constant (A), and friction coefficient (μ) of PU elastomer, soft PUA, and hard PUA. The three materials are denoted as PU, s-PUA, and h-PUA, respectively.

Material	E	A	μ
PU	≈3 Mpa	5.71×10^{-20} J	0.12
s-PUA	≈19.8 Mpa	2.09×10^{-20} J	0.04
h-PUA	≈350 Mpa to 10 Gpa	1.78×10^{-20} J	0.08

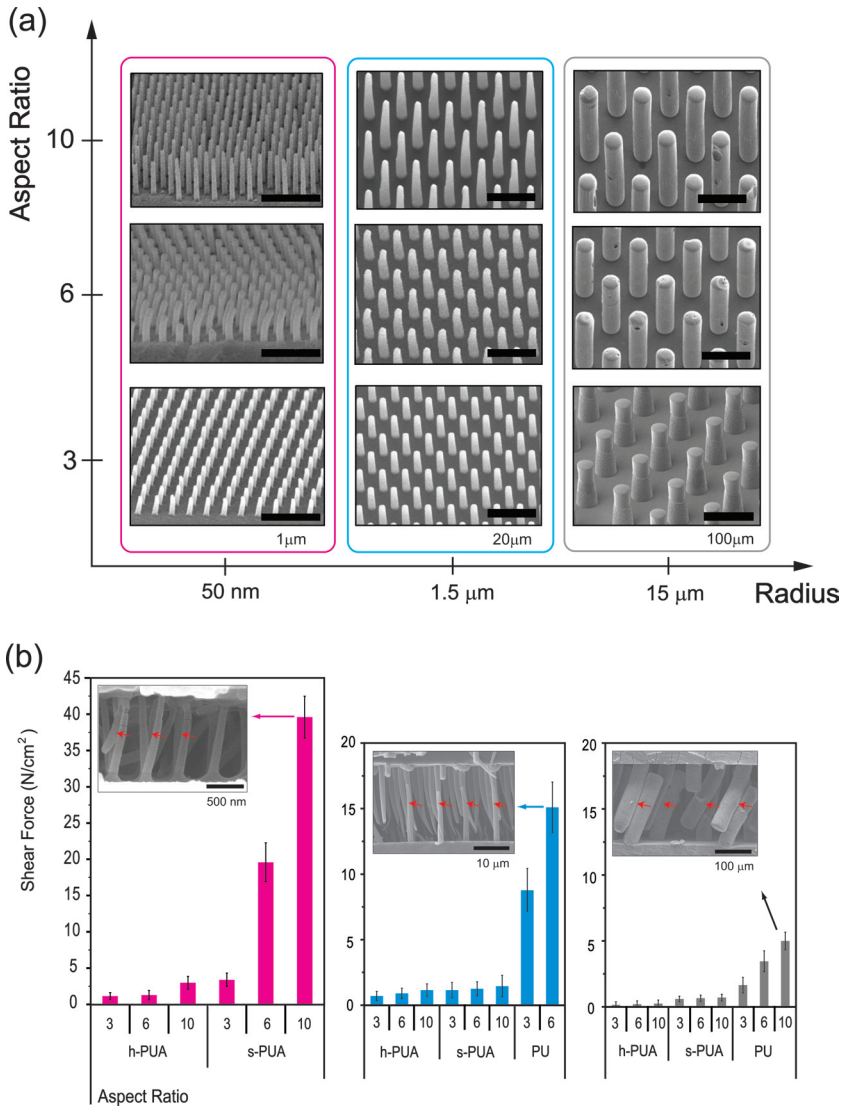

Figure 2. a) Micro- and nanohairs of different radius (50 nm, 1.5 μm, and 15 μm) with three ARs (3, 6, and 10). For consistency, all of the hairy structures have the same spacing ratio of 3 with the hexagonal packing geometry. b) Shear adhesion forces of the hairy structures (radius: 50 nm, 1.5 μm, and 15 μm) with three ARs (3, 6, and 10). The red arrows in the inset cross-sectional SEM images indicate the locations of interlocking contacts.

adhesion over >300 cycles without significant reduction in adhesion strength (10 nm Pt thickness). The SEM images also support this finding; no significant structural collapse was observed in the presence of a thin Pt coating (see Supporting Information Figure S4).

To gain further understanding on multiscale van der Waals force-assisted interlocking, we derive a simple theory based on force balance and hair-merging probability. The hair-to-hair interlocking contact would occur in a series of steps (see Supporting Information Figure S5). When the hairs are brought in contact by an applied load, they are attracted by van der Waals forces,[21] forming a reversible contact between the two layers. Here, the force between the hairs can be written as $F_{vdw} = A\sqrt{R}\,l/(16\,D^{2.5})$,[19] in which A is the Hamaker constant, R is the hair radius, D is the distance between hairs, and l is the overlap length. The Hamaker constants of PU elastomer, s-PUA, and h-PUA were calculated to be 5.71×10^{-20} J (A_{PU}), 2.09×10^{-20} J ($A_{s\text{-}PUA}$), and 1.78×10^{-20} J ($A_{h\text{-}PUA}$), respectively (Table 1). In the course of forming an interlocking contact, the deflection of hairs costs the bending energy of the upper and lower vertical hairs, which is given by $F_{def} = 48EID/\{(2l_0 - l)^2(4l_0 + l)\}$ where I is the moment of inertia ($I = \pi R^4/4$), l_0 is the total length of hairs, and E is the elastic modulus of the polymer material (see Table 1). It is noted that the original beam deflection equation was modified by using the overlap distance l. Then, the maximum pairing distance between hairs, D_p, can be determined by equating the van der Waals and hair deflection forces. Since two hairs are involved in a single contact, one can assume $F_{vdw}(D_p) = 2F_{def}(D_p)$, which gives

$$D_p \approx 0.475\gamma_{aspect}\left(R\gamma_{aspect}\right)^{1/7}(A/E)^{2/7} \quad (1)$$

where γ_{aspect} is the AR of hairs ($= l_0/2R$) and the constant 0.475 originates from the average overlap length of $0.7l_0$ from our experimental observations. Therefore, the interlocking probability increases with the increase of the AR, hair length, and van der Waals forces, whereas it decreases with the increase of the modulus of material (see Supporting Information Figure S5).

Once the initial contact is made, the maximum displacement of hairs D_s prior to separation can be derived based on the force balance and friction law (see Supporting Information). Since the hairs are now merged, the van der Waals force is described by $F_{vdw} = A\sqrt{R}\,l/(16\,D_0^{2.5})$,[21] in which the cut-off gap distance between hairs D_0 is assumed to be 0.4 nm.[19] After plugging in the tilting angle (θ) of $1.276D_s/l_0$ and applying the force balance $F_{def}\sin\theta = \mu(F_{vdw} - F_{def}\cos\theta)$ with algebraic manipulation, one can have

$$D_s \approx 0.783\mu\,\gamma_{aspect}R\left[\sqrt{\frac{0.376}{D_0^{2.5}}\frac{\gamma_{aspect}^3}{R^{0.5}}\frac{A}{\mu E}+1}-1\right] \quad (2)$$

where μ is the frictional coefficient of each material (Table 1). Therefore, the maximum deflection is linearly proportional to $R\gamma_{aspect}$(or l_0), which is readily understood in terms of geometrical considerations. Additionally, the theoretical shear adhesion force per single hair can be predicted based on the same formulation, yielding $F_{shear} = F_{vdw}\cos\theta$. The maximum shear adhesion is predicted to be ≈65 N m^{-2} for the nanohairs of 50 nm radius and 1 μm height and ≈29 N cm^{-2} for the microhairs of 1.5 μm radius and 18 μm height, respectively, which are approximately 1.5 to 2 times higher than the experimental data shown in

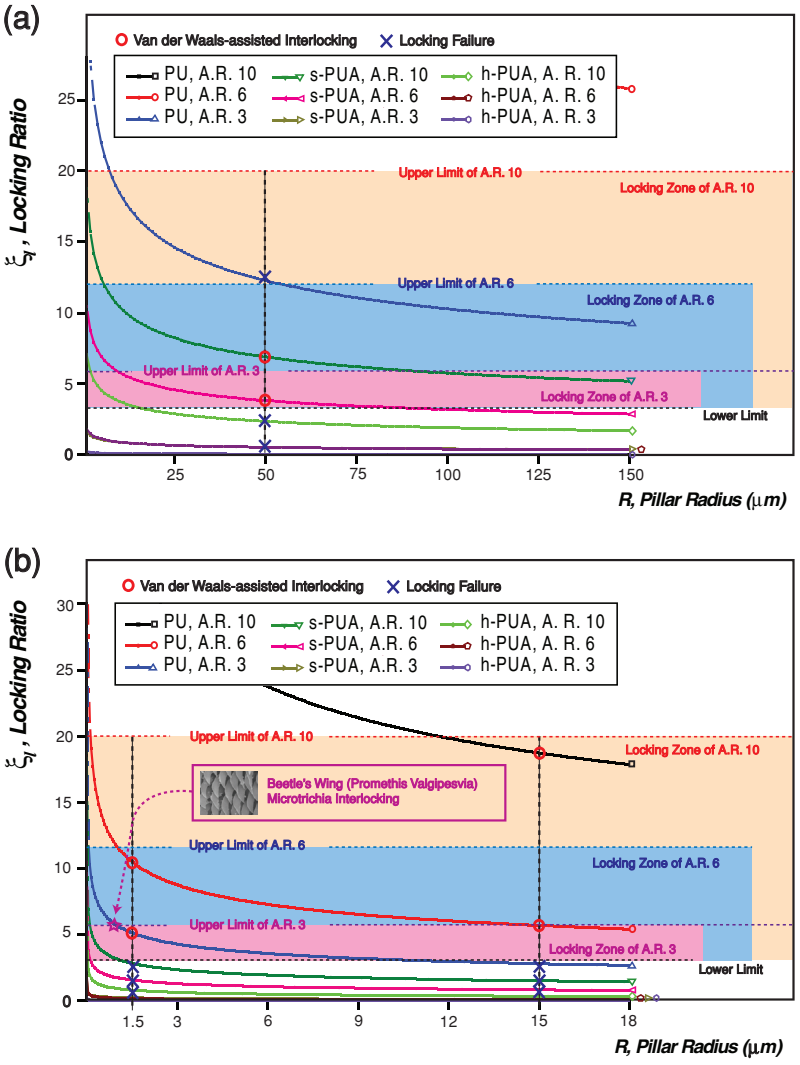

Figure 3. Interlocking operating zones for 50 nm radius and 1 μm height hairs (a) and for 1.5 μm and 15 μm radius microhairs (b). The lower and upper limits are marked as dotted lines with different colors for each AR.

Figure 2b. It appears that the interlocking contact is not complete, in part due to misalignment of upper and lower hair arrays and some structural defects.

To judge whether interlocking would take place or not, it is useful to set lower and upper limits of locking criterion. For the hexagonal unit cell arrays with a certain spacing ratio ($\gamma_{spacing} = d/2R$), it can be assumed that D_s should exceed the unit cell distance to contact the neighboring hairs even in a misaligned state. Thus, the lower limit of interlocking setting is derived from the condition where the area ratio (ϕ_{area}) should be larger than unity:

$$\phi_{area} = \frac{\pi(R + D_s)^2}{4R^2(\gamma_{spacing} + 1)\sin\alpha} > 1 \quad (3)$$

Here, $\gamma_{spacing}$ is the same at 3 and the arrangement angle α is 60° for the hexagonal packing geometry. This lower limit accounts for the maximum hair-merging probability, even in a misaligned state. Next, the upper limit is given by the geometric consideration, such that the interlocking ratio $\xi_l (= D_s/R)$ should be less than double the interspacing ratio so as to prevent clumping with the bottom substrate. Therefore one may write

$$\sqrt{\frac{4(\gamma_{spacing} + 1)\sin\alpha}{\pi}} - 1 < \xi_l < 2\gamma_{aspect} \quad (4)$$

After inserting appropriate values into the parameters in Equations 3 and Equation 4, it follows that $3.20 < \xi_l < 2\gamma_{asp}$. **Figure 3** shows the plots of ξ_l versus the change in hair radius for each experimental set with the corresponding material properties shown in Table 1. The lower and upper limits of interlocking are marked as dotted lines with different colors for each AR. As can be seen from the figure, the existence of van der Waals force-assisted interlocking can be predicted by comparing the interlocking zones with the plots based on Equation 4, which is also in excellent agreement with our experimental observations in Figure 2b as well as the wing locking device of the beetle (*Promethis valgipes*) in Figure 1. It is noted that the interlocking zone becomes wider as the AR increases for given material rigidity, suggesting that the structures of high AR are advantageous for efficient interlocking.

In summary, we have presented a robust, reversible interlocking system using regularly arrayed, high-AR polymer fibers inspired from the wing-locking device of beetles. Our experimental and theoretical studies demonstrate that the interlocking is mediated by attractive van der Waals forces among high-AR hairy structures, resulting in a very high interlocking force in the shear direction (≈40 N cm^{-2}) and easy life-off in the normal direction. In contrast to other reversible binding systems, the current interlocking mechanism does not involve any complicated physical structures (e.g., hooks or loops) or surface chemical moieties, allowing for an simple, yet efficient, route to reversible interlocker in a noiseless and cost-effective manner. A simple theory was developed on the basis of force balance and hair-merging probability, which is capable of explaining the maximum shear adhesion and operating zones for various geometrical and material parameters.

Experimental Section

The silicon masters with micro- and nanoholes were prepared by photolithography and subsequent reactive ion etching. The masters were treated with a fluorinated self-assembled monolayer (SAM) solution ((tridecafluoro-1,1,2,2-tetrahydrooctyl)-trichlorosilane [$CF_3(CF_2)_5CH_2CH_2SiCl_3$] (FOTCS), Gelest Corp.) diluted to 0.03 M in anhydrous heptane (Samchon Corp.) in an Ar chamber. The surface-treated masters were annealed at 120 °C for 20 min. Then, drops of

PU elastomer (PU), or PUA pre-polymers (s-PUA; PUA MINS 311 RM, h-PUA; PUA MINS 301 RM) purchased from the Minuta Tech, Korea, were dispensed onto the master and a polyethylene teraphthalate (PET) film (50 μm) was slightly pressed against the liquid drop for it to be used as a supporting backplane. After preparing a polymer replica by UV exposure and mold removal, the PUA replica was additionally exposed to UV for several hours for complete curing. Details on the synthesis and characterization of the PUA polymers can be found elsewhere.[16] For the fabrication of hair arrays, three types of micro- and nanoscale pillar structures were used with the above three polymer materials: i) 50 nm radius nanohairs of 300 nm, 600 nm, and 1 μm height, ii) 1.5 μm radius with 9 μm, 18 μm, and 27 μm height, and iii) 15 μm radius with 90 μm, 180 μm, and 270 μm height. In total, 27 experimental sets were prepared and used for SEM measurements and adhesion tests.

Supporting Information

Supporting Information is available from the Wiley Online Library or from the author.

Acknowledgements

C.P. and T.K. contributed equally to this work. This work was supported by the National Research Foundation (NRF) of Korea grant (No. 20110017530), WCU (World Class University) program (R31-2008-000-10083-0), and Basic Science Research Program (2010-0027955). This work was supported in part by the Global Frontier R&D Program on Center for Multiscale Energy System funded by the NRF and Institute of Advanced Machinery and Design (IAMD) and Engineering Research Institute of Seoul National University.

Received: August 7, 2011
Revised: September 22, 2011
Published online: December 19, 2011

[1] D. H. Kim, N. S. Lu, R. Ma, Y. S. Kim, R. H. Kim, S. D. Wang, J. Wu, S. M. Won, H. Tao, A. Islam, K. J. Yu, T. I. Kim, R. Chowdhury, M. Ying, L. Z. Xu, M. Li, H. J. Chung, H. Keum, M. McCormick, P. Liu, Y. W. Zhang, F. G. Omenetto, Y. G. Huang, T. Coleman, J. A. Rogers, *Science* **2011**, *333*, 838.
[2] K. Autumn, M. Sitti, Y. C. A. Liang, A. M. Peattie, W. R. Hansen, S. Sponberg, T. W. Kenny, R. Fearing, J. N. Israelachvili, R. J. Full, *Proc. Natl. Acad. Sci. USA* **2002**, *99*, 12252.
[3] M. Sitti, R. S. Fearing, *J. Adhes. Sci. Technol.* **2003**, *17*, 1055.
[4] L. F. Boesel, C. Greiner, E. Arzt, A. del Campo, *Adv. Mater.* **2010**, *22*, 2125.
[5] M. K. Kwak, C. Pang, H. E. Jeong, H. N. Kim, H. Yoon, H. S. Jung, K. Y. Suh, *Adv. Funct. Mater.* **2011**, *21*, 3606.
[6] L. P. Lee, R. Szema, *Science* **2005**, *310*, 1148.
[7] G. Q. Liang, X. L. Zhu, Y. G. Xu, J. Li, S. Yang, *Adv. Mater.* **2010**, *22*, 4524.
[8] Y. M. Zheng, H. Bai, Z. B. Huang, X. L. Tian, F. Q. Nie, Y. Zhao, J. Zhai, L. Jiang, *Nature* **2010**, *463*, 640.
[9] F. Xia, L. Jiang, *Adv. Mater.* **2008**, *20*, 2842.
[10] S. S. G. Matthias scherge, *Biological Micro- and Nano- tribology Nature's Solutions*, Springer, Berlin **2001**.
[11] G. Mestral, *US patent 3009235,* **1961**.
[12] S. N. Gorb, *Int. J. Insect Morphol.* **1998**, *27*, 205.
[13] H. Ko, J. Lee, B. E. Schubert, Y. L. Chueh, P. W. Leu, R. S. Fearing, A. Javey, *Nano Lett.* **2009**, *9*, 2054.
[14] Y. Zhao, T. Tong, L. Delzeit, A. Kashani, M. Meyyappan, A. Majumdar, *J. Vac. Sci. Technol. B* **2006**, *24*, 331.
[15] K. Autumn, A. M. Peattie, *Integr. Comp. Biol.* **2002**, *42*, 1081.
[16] S.-J. Choi, H. N. Kim, W. G. B. Bae, K.-Y. Suh, *J. Mater. Chem.* **2011**, *21*, 11.
[17] H. E. Jeong, J. K. Lee, H. N. Kim, S. H. Moon, K. Y. Suh, *Proc. Natl. Acad. Sci. USA* **2009**, *106*, 5639.
[18] Velcro, www.torstamp.com/Brochures/BR-122.pdf, (accessed November 2011).
[19] D. Leckband, J. Israelachvili, *Q. Rev. Biophys.* **2001**, *34*, 105.
[20] T. I. Kim, H. E. Jeong, K. Y. Suh, H. H. Lee, *Adv. Mater.* **2009**, *21*, 2276.
[21] J. N. Israelachvili, *Intermolecular and surface forces* Academic Press, San Diego **1991**.